Матеріали XXIII Міжнародної науково-практичної конференції «Екологія. Людина. Суспільство» (м. Київ, Україна, 7 грудня2023 р.)

Handbook of the XXIII International Science Conference «Ecology. Human. Society» (December 7, 2023 Kyiv, Ukraine)

ISSN (Online) 2710-3315
DOI: https://doi.org/10.20535/EHS2710-3315.2023.290851

УДК 661.097.3; 542.978, 697.94; 544.478.023.57; 544.478.41

APPLICATION OF FERRIFEROUS HYDROSOL FOR CO_2 CAPTURE

Ihor BYCHKO[1], Andriy TRYPOLSKYI[1], Victoria KOVBASIUK[2]

[1]*L.V. Pisarzhevskii Institute of Physical Chemistry of the National Academy of Sciences of Ukraine,* Nauky Ave., 31, Kyiv, Ukraine
[2]*Igor Sikorsky Kyiv Polytechnic Institute*
Beresteiskyi ave., 37, Kyiv, Ukraine
e-mail: igorbychko@ukr.net

Introduction. The demand for strategies to reduce global atmospheric concentrations of greenhouse gases is considered one of the main tasks for 21 century. The capture and sequestration of carbon dioxide, the predominant greenhouse gas, is a central strategy of these initiatives. Carbon capture and storage (CCS) schemes embody a group of technologies for the capture of CO_2 from power plants, followed by compression, transport, and permanent storage [1]. The main technologies of CO_2 capture are based on the processes of absorption-desorption in absorbing solutions, membrane separation, adsorption, and mineralization [2, 3, 4]. Technology for the use of absorbent solutions, in particular amines, is common in the industry, while other technologies are in the concept or pilot stages [5]. Carbon capture and utilization (CCU) is an alternative approach to reducing CO_2 emissions [6]. CCU can be realized by chemical fixation through the conversion of CO_2 into fuels, commodity chemicals, construction materials, or mineral carbonates represents another promising alternative for CO_2 capture. Particularly, CO_2 may be considered as feed to produce fuels such as methanol, formic acid, dimethyl carbonate, methyl formate, and higher hydrocarbons, as well as polymeric materials and pharmaceutical chemicals [7].

The carbonate cycle is a novel concept for CCU technology that is based on the adsorption of CO_2 by metal oxides with further transportation and degassing with the regeneration of initial oxide [8]. In metal carbonate decarboxylation, the reaction conditions, especially the nature of the gas atmosphere, play a crucial role in the course of the reaction. If carried out in a reducing atmosphere of hydrogen, the decomposing of carbonate combines with chemical transformations of CO_2 into valuable products. The main advantage of the carbonate method is the possibility of the transformation of carbon dioxide into hydrocarbons using hydrogen [9]. The use of "green" hydrogen in the hydrogenation of carbonates predicts a closed carbon cycle. Iron oxides are a leading candidate for this technology due to the high dissemination and low cost of iron. Iron is an industrial catalyst of Fisher-Tropsh synthesis, a process of obtaining synthetic fuels from synthesis gas [10]. It could be expected, that selection of experimental conditions allows obtaining not only methane and carbon monoxide, as a reaction product, but also higher hydrocarbons. Iron carbonate also can be utilized as inorganic pigment that provides a brown and red-brownish coloring.

As reported in the literature, only Fe^{2+}, mainly in the form of FeO, applies to CO_2 capture, while Fe^{3+} is unsuitable for this approach due to its inability to form carbonates. However, FeO is a quasi-stable oxide that disproportionates producing Fe and Fe_3O_4 [11]. Therefore, iron in the form of Fe_3O_4, or a mixture of iron oxides/hydroxides is suitable for large-scale adsorption of CO_2 [12]. Adsorption capacity and kinetics can be increased by the use of a water suspension. The commercial products of

suspension of iron oxides/hydroxides named ferryferrohydrosol (FFH) which is used for purification of waste water, is also predicted to be a perspective adsorbent for CO_2. FFH is a colloidal suspension of two- and three-valence iron hydrated compounds, used as a reagent for wastewater pollutants binding. The method of manufacturing FFH is apparently simple and based on the electrolysis of iron and steel stamping waste. Predicted, that electrolysis of steel leads to a formation of iron-containing oxide-hydroxide nanoparticles that shows a tendency of coagulation into coarse bunches, and the formation of agglomerates with a size of several micrometers. Formed FFH characterizes by enhanced sorption capacity, particularly due to the developed specific surface of iron-containing particles, that can achieve 400 m².

The presented work is dedicated to the assessment of the possibility of capturing CO_2 using the FFH suspension as a perspective product for cleaning concentrated exhaust gases produced by fossil fuel-based enterprises.

Methods. Samples of FHH were provided by the manufacturer, the INECO company (Innovation Ecology), Vilnius, Republic of Lithuania. It was provided 3 samples that contains 40g/l of FFH with 4g/l of NaCl (FFH-NaCl), 30g/l of FFH with 4g/l of Na_2SO_4 (FFH-Na_2SO_4), and 40g/l of FFH with 4g/l of Na_2SO_4 and 2 g/l of a compound (FFH-Na_2SO_4+). Also, commercial magnetite Fe_3O_4 325 mesh (≈ 45 μm) from "Thermo scientific" was used as a sample for comparison. The structure of the samples were characterized by Raman spectroscopy. Raman spectra were performed a HORIBA Jobin-Yvon T64000 spectrometer using exciting Ar-Kr laser radiation at a wavelength of 488 nm and a power of 100 mW. Fourier transform infrared (FTIR) spectra were obtained using a Spectrum-One spectrometer (PerkinElmer). The dynamic light scattering (DLS) measurements were made with a Malvern Zetasizer Nano S, using a 633 nm HeNe laser at 4 mW. Aqueous suspensions of initial FFH, and FFH after CO_2 adsorption were tested in quartz cuvettes having a 10 mm path length. The analysis was operated in backscatter mode at an angle of 173º. Samples were equilibrated at 25 ºC for 30 min before measurement. The concentration of FFH in water was 1 mg/ml. The capacity of FFH for CO_2 adsorption was determined using a volumetric method. The flask with a sample was connected to a cuvette filled with dibutylphtalate. The duration of each adsorption experiment was at least 30 minutes.

Results and Discussion. Figure 1 presents FTIR and Raman-spectra of initial FFH samples, commercial Fe_3O_4, and corresponding samples after CO_2 adsorption. A comparison of spectra of initial FFH shows that spectra of FFH-Na_2SO_4+ and FFH-Na_2SO_4 are very similar, while the spectrum of FFH-NaCl shows a noticeable difference. Bands ad 340 cm^{-1}, 495 cm^{-1}, and a broad band at 685cm-1 in combination with a band at 1395 cm^{-1} show, that the main phase of FFH-Na_2SO_4+ and FFH-Na_2SO_4 is maghemite - γ-Fe_2O_3 [13]. The spectra of FFH-NaCl present the same bands combined with two intense bands at 220 cm^{-1} and 280 cm^{-1} which are corresponds to hematite - α-Fe_2O_3 [14]. Raman spectra of magnetite contains a weak band at 540 cm^{-1} and strong band at 662 cm^{-1}, which are typical bands of magnetite [15].

A comparison of Raman-spectra of initial FFH samples and FFH after CO_2 adsorption shows only a slight decrease of band intensity. The main Raman bands of siderite appear at 190 cm^{-1}, 290 cm^{-1}, and the most intense band at 1100 cm^{-1} [16]. Therefore, CO_2 adsorption does not lead to the appearance of detectable bands of siderite, which can be caused by a low concentration of formed siderite. Raman spectra of magnetite after CO_2 adsorption are almost identical to the initial Fe_3O_4.

Bands at 570-580 cm^{-1} in the FTIR spectra correspond to a Fe–O stretching mode of the tetrahedral and octahedral sites of Fe_3O_4 in Fe_3O_4, and FFH samples. Weak band 800 cm^{-1} can be attributed to a –OH stretching vibration of α-FeOOH [17, 18]. Bands with low intensity near 1000 cm^{-1} are the bending vibration of –OH modes in γ-FeOOH and a broad peak at 1100 cm^{-1} is the bending vibration of OH modes in δ-FeOOH. Peaks at 1300–1500 cm^{-1} could be related to the stretching vibration band

of the CO_3 group that mainly arises from the contamination of solutions by atmospheric carbon dioxide [19]. A pronounced band at ~1620–1630 cm^{-1} is related to the H–O–H bending of water.

Adsorption of CO_2 leads to the appearance of the band at 470 cm^{-1} in FFH-NaCl(CO_2) and FFH-Na_2SO_4(CO_2) as well as a new band at 440 cm^{-1} in Fe_3O_4-CO_2, which corresponds to metal-oxygen vibration modes if maghemite [20]. The spectra of Fe_3O_4-CO_2 contain a doubled band at 520–750 cm^{-1} which is a result of the combination of Fe–O stretching mode of Fe_3O_4 and γ-Fe_2O_3. The spectra of Fe_3O_4(CO_2) contain two intense bands at 900-1100 cm^{-1} that era attributed to surface OH groups in magnetite (960 cm^{-1}) and maghemite (1080 cm^{-1}). There is a significant increase in the intensity of

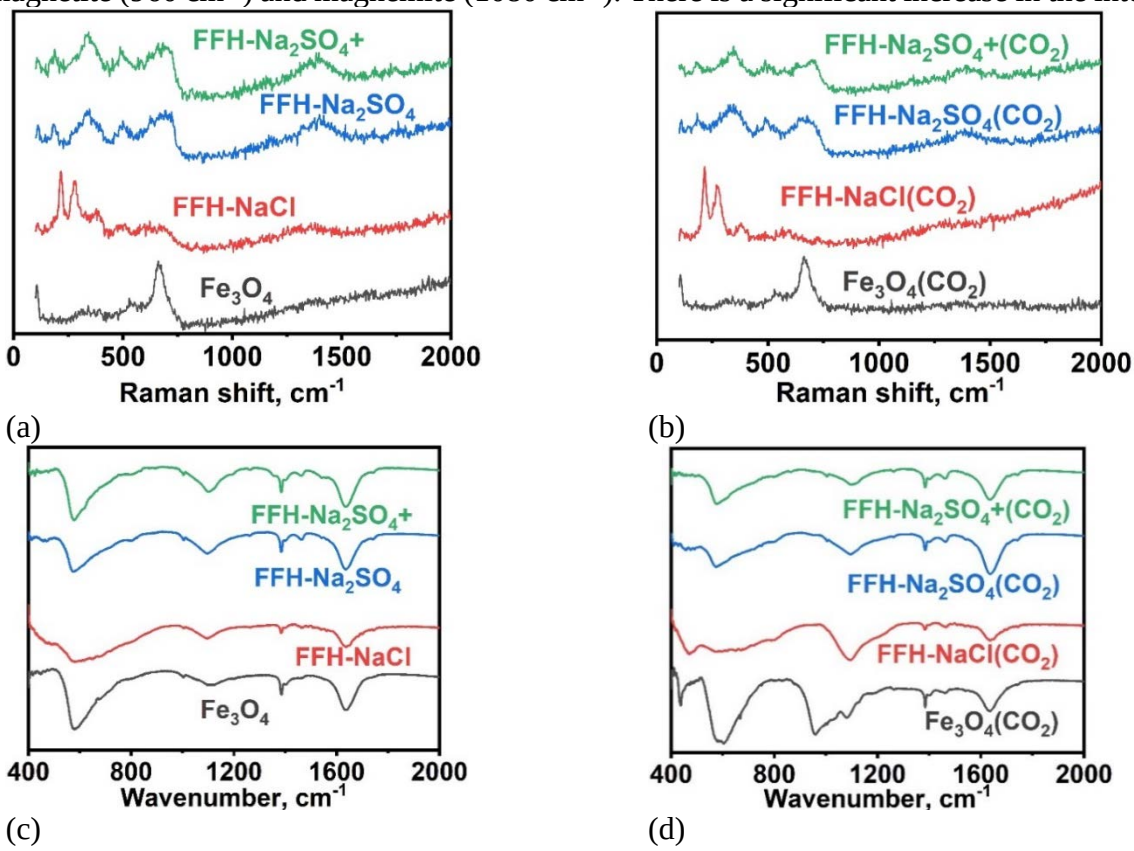

Figure 1. Raman (a) and FTIR (b) spectra of initial FFH samples, commercial Fe_3O_4, and Raman (c) and FTIR (d) spectra of corresponding samples after CO_2 adsorption.

the band at 1100 cm-1 for the FFH-NaCl(CO_2) sample in comparison with the initial FFH-NaCl. This result indicates an increase in the content of the phase of γ-FeOOH due to CO_2 adsorption. Adsorption of CO2 does not lead to significant changes in the FTIR spectra of FFH-Na_2SO_4(CO_2) and of FFH-Na_2SO_4+(CO_2) compared with initial samples.

Table 1. Average particles size of initial FFH samples and FFH after adsorption of CO_2.

№	Sample	Average particles size, μm
1	FFH-Na_2SO_4+	6.5±0.2
2	FFH-Na_2SO_4	3.4±0.1
3	FFH-NaCl	4.7±0.1
4	FFH-Na_2SO_4+(CO_2)	2.8±0.1
5	FFH-Na_2SO_4(CO_2)	2.7±0.1
6	FFH-NaCl(CO_2)	2.6±0.1

Table 1 presents the average particles size of initial FFH samples and FFH samples after CO_2 adsorption determined by DLS. Obtained results show that FFH contains particles of a size of several micrometers. The smaller particles of 2.5 micrometers contain FFH-NaCl, while FFH-Na_2SO_4+ contains the larger particles of 6.5 micrometers. Adsorption of CO_2 decreases the average particle size for all samples to a size close to 2.7 micrometers. This result indicates that the adsorption of CO_2 leads to breaking the bonds in iron-containing particles, probably hydrogen bonds that result in the grinding of the particles agglomerates to smaller initial particles. Therefore, analysis shows, that FFH contains a suspension of iron-containing particles with a size of several micrometers which are a mix of oxides and hydroxides of Fe^{2+} and Fe^{3+}. The main crystalline phases of these particles are maghemite, hematite, and magnetite with a significant content of their hydrated forms. It can be speculated, that the main amount of CO_2 adsorbs by Fe in amorphous forms, which are the major phase of Fe in FFH. Adsorption of CO_2 has a limited effect on the transformation of crystalline phases, which consists in the transition of the magnetite phase to maghemite. While the amorphous phase of particles adsorbs CO_2 by surface OH-groups and oxides forming nanostructures containing carbonates and hydroxycarbonates that aggregate into particles with sizes near 2.5-3 micrometers.

Table 2 presents experimental results of the adsorption of CO_2 by FFH samples. At 20 ºC FFH adsorbs 3-4.5 liters or 6-8.5 g of CO_2. The ultimate amount of adsorbed CO_2 by iron oxide/hydroxide systems can be calculated according to the ratio, where 1 mole of Fe adsorbs 1 mole of CO_2. This proportion follows from the equation $FeO+CO_2=FeCO_3$. Therefore, 1 liter of FFH, which contains 40 g of Fe, can adsorb 31.4 g or 16 liters of CO_2. Adsorption of CO_2 by water is negligible due to the influence of electrolyte and solid particles, which dramatically reduce the adsorption capacity of the water. Therefore, according to this approach, the adsorption capacity of FFH samples is 8.5-14.5% of the theoretical value. This indicates that only a limited amount of iron compounds adsorbs CO_2. The adsorption capacity determined experimentally is lower than the theoretic value, which can be caused by the inaccessibility of the inner part of particles to the CO_2 at 20 ºC. The high content of Fe^{3+} is another reason of the depressed capability of FFH towards the adsorption of CO_2. Adsorption of CO2 by magnetite is negligible, that is a consequence of a very low specific surface due to large particles size.

Table 2. The density of FFH samples, the amount of adsorbed CO_2 by FFH samples at 20º C, and the amount of adsorbed CO_2 relative to the theoretic value obtained from the proportion of (1 mole CO_2)/(1 mole FeO).

Sample	**Density, g/cm^3**	**liter(CO_2)/liter(FFH)**	**g(CO_2)/kg(FFH)**	**g(CO_2)/g(Fe)**	**% from theory**
FFH-Na_2SO_4+	1.06	3.1	5.8	0.15	8.5
FFH-Na_2SO_4	1.04	3.9	7.4	0.26	14.5
FFH-NaCl	1.05	4.3	8	0.21	12
*Fe_3O_4	-	<0.01	<0.1	<0.001	<0.001

* Experiment of CO_2 adsorption by Fe_3O_4 was provided using a suspension of 40g Fe_3O_4 and 4g NaCl in 1 liter of water

Comparison of data presented in Table 1 and Table 2 shows, that amount of adsorbed CO_2 increases with a decrease of particles size of FFH. This result indicates that the influence of particles

size on the adsorption capacity is very significant. Therefore, a strategy for the creation of a highly effective FFH is not only to obtain a FFH with a high content of Fe^{2+} but also with a small size of iron-containing particles. Also, it can be concluded that the main role of electrolytes is the determination of particles size of FFH, and the influence of various electrolytes on differences in phase composition, the ratio of Fe^{2+}/Fe^{3+}, and, as a consequence, the adsorption capacity is negligible.

The alternative approach, which is based on the study of model systems of iron oxides, shows that at room temperature is mainly observed physical adsorption of CO_2 on all types of iron oxides. It was shown, that the degree of surface hydroxylation plays a decisive role in the adsorption of CO_2 on the surface of iron oxides, which leads to the formation of adsorbate forms identified as surface bicarbonates. Adsorbed CO_2 over a long period of time can transform into a chemisorbed form with the formation of carbonates and bicarbonates. However, such a process occurs only in the presence of Fe^{2+} [21, 22, 23]. According to this, a developed surface of iron oxides is required for an increase in the absorption capacity. The maximum amount of $3.01*10^{-3}$ gCO_2/g of absorbed CO_2 was observed for Fe_2O_3. The adsorption of CO_2 by a biochar/Fe oxyhydroxide sorbent of 0.16 gCO_2/g at 25 °C was achieved [21].

Following this approach obtained values of adsorbed CO_2 by FFH allow the determination of the specific surface area (SSA) of iron particles which can be calculated using:

$$S = q \cdot \sigma_0 \cdot N_A$$

where, q is the adsorption capacity of CO_2 (mol/g), σ_o is the area claimed by an adsorbed molecule of CO_2 (0.109×10^{-18} m^2), and N_A is Avogadro's number (6.022×10^{23} mol^{-1}). The obtained result of the SSA of iron in FFH gives 220-390 m^2/g. Comparing the values of SSA and particles size obtained by DLS confirms that the iron-containing oxide particles in the samples are porous agglomerates of smaller, mostly amorphous nanoparticles with a highly developed surface.

Conclusions. The possibility of applying FFH for the absorption of CO_2 from concentrated exhaust gases was demonstrated. It was shown, that the structure of FFH is a suspension of iron-containing nanoparticles which are a mix of oxides and hydroxides of Fe^{2+} and Fe^{3+}. These nanoparticles are agglomerated in larger particles with a size of several micrometers. The main crystalline phases of these particles are maghemite, hematite, and magnetite with significant content in their hydrated forms. FFH samples have a developed surface in the range of 200-400 m^2/g. The absorption capacity for CO_2 of 0.26 $g(CO_2)/g(Fe)$ at room temperature was shown. A high absorption capacity of FFH can be associated with a highly developed surface area of the samples and a high degree of surface hydroxylation. Therefore, the use of FFH to absorption of CO_2 from concentrated exhaust gases has significant advantages over solid sorbents.

Acknowledgments. This work was provided with the support of The EUREKA Network, project E! 13401 FFH-CO_2.

References:

1. Arshad Raza, Raoof Gholami, Reza Rezaee, Vamegh Rasouli, Minou Rabiei. (2019). Significant aspects of carbon capture and storage – A review. Petroleum. 5(4). pp. 335-340.
2. Brunetti A., Scura F., Barbieri G., Drioli E. (2010). Membrane technologies for CO_2 separation. Journal of Membrane Science. 359(1–2), pp. 115-125.
3. Masoud Mofarahi, Fatemeh Gholipour. (2014). Gas adsorption separation of CO_2/CH_4 system using zeolite 5A. Microporous and Mesoporous Materials. 200. pp. 1-10.
4. Zhang S., DePaolo D.J. (2017). Rates of CO_2 Mineralization in Geological Carbon Storage. Accounts of chemical research. 50(9). pp. 2075-2084.

5. Lalit A. Darunte, Krista S. Walton, David S. Sholl, Christopher W. Jones. (2016). CO_2 capture via adsorption in amine-functionalized sorbents. Current Opinion in Chemical Engineering. 12. pp. 82-90.

6. Ikhlas Ghiat, Tareq Al-Ansari. (2021). A review of carbon capture and utilisation as a CO_2 abatement opportunity within the EWF nexus. Journal of CO_2 Utilization. 45. 101432.

7. Anwar M.N., Fayyaz A., Sohail N.F., Khokhar M.F., Baqar M., Yasar A., Rasool K., Nazir A., Raja M.U.F., Rehan M., Aghbashlo M., Tabatabaei M., Nizami A.S. (2020). CO_2 utilization: Turning greenhouse gas into fuels and valuable products. Journal of Environmental Management. 260. 110059.

8. Lux S., Baldauf-Sommerbauer G., Siebenhofer M. (2018). Hydrogenation of Inorganic Metal Carbonates: A Review on Its Potential for Carbon Dioxide Utilization and Emission Reduction. ChemSusChem. 11(19). pp. 1864-5631.

9. Bychko I.B., Kovbasiuk V.I., Trypolskyi A.I., Ivanchuk V.Y., Strizhak P. E. (2021). Low-Temperature Hydrogenation of Iron Carbonate Followed By Production of C4-C6 Hydrocarbons. Theoretical and Experimental Chemistry. 57. pp. 351–357.

10. Frątczak J., de Paz Carmona H., Tišler Z., Hidalgo Herrador J.M., Gholami Z. (2021). Hydrocracking of Heavy Fischer–Tropsch Wax Distillation Residues and Its Blends with Vacuum Gas Oil Using Phonolite-Based Catalysts. Molecules. 26(23):7172.

11. Eduin Yesid Mora Mendoza, Armando Sarmiento Santos, Enrique Vera López, Vadym Drozd, Andriy Durygin, Jiuhua Chen, Surendra K. Saxena. (2019). Iron oxides as efficient sorbents for CO_2 capture. Journal of Materials Research and Technology. 8(3). pp. 2944-2956.

12. Mora Mendoza E., Sarmiento Santos A., Vera E., Drozd V., Durygin A., Chen J., Saxena S. (2019). Siderite Formation by Mechanochemical and High Pressure–High Temperature Processes for CO_2 Capture Using Iron Ore as the Initial Sorbent. Processes. 7. 735.

13. de Faria D. L. A., Venâncio Silva S., de Oliveira M. T. (1997). Raman microspectroscopy of some iron oxides and oxyhydroxides. Journal of Raman Spectroscopy. 28(11). pp. 873-878.

14. Shim Sang-Heon, Duffy Thomas S. (2002). Raman spectroscopy of Fe_2O_3 to 62 GPa. American Mineralogist. 87(2-3). pp. 318-326.

15. Chicot Didier, Francine Roudet, Lepingle V., Louis Ghyssels. (2009). Strain gradient plasticity to study hardness behavior of magnetite (Fe_3O_4) under multicyclic indentation. Journal of Materials Research. 24. pp. 749-759.

16. Tuller H.L., Nowick, A.S. (1977). Small Polaron Electron Transport in Reduced CeO_2 Single Crystals. J. Phys. Chem. Solids. 38, pp. 859-867.

17. Stoia Marcela, Istratie Roxana, Păcurariu C. (2016). Investigation of magnetite nanoparticles stability in air by thermal analysis and FTIR spectroscopy. Journal of Thermal Analysis and Calorimetry. 125.

18. Xing B., Graham N., Yu W. (2020). Transformation of siderite to goethite by humic acid in the natural environment. Commun Chem. 3. 38.

19. Kumar Rohit, Sakthivel R., Behura Reshma, Mishra B.K., Das D. (2015). Synthesis of magnetite nanoparticles from mineral waste. Journal of Alloys and Compounds. 645. pp. 398-404.

20. Siyaram Sankadiya, Nidhi Oswal, Pranat Jain, Nitish Gupta. (2016). Synthesis and characterization of Fe_2O_3 nanoparticles by simple precipitation method. AIP Conf. Proc. 1724(1). 020064.

21. Xiaoyun Xu, Zibo Xu, Bin Gao, Ling Zhao, Yulin Zheng, Jinsheng Huang, Daniel C.W. Tsang, Yong Sik Ok, Xinde Cao. (2020). New insights into CO_2 sorption on biochar/Fe oxyhydroxide composites: Kinetics, mechanisms, and in situ characterization. Chemical Engineering Journal. 384. 123289.

22. Xiaoke Li, Joachim A. Paier. (2020). Vibrational properties of CO_2 adsorbed on the Fe_3O_4 (111) surface: Insights gained from DFT. The Journal of chemical physics.152(10). 104702.

23. Sergio Tosoni, Davide Spinnato, Gianfranco Pacchioni. (2015). DFT Study of CO_2 Activation on Doped and Ultrathin MgO Films. The Journal of Physical Chemistry C. 119(49). pp. 27594-27602.